Frontiers in Laboratory Medicine xxx (2017) xxx–xxx

Contents lists available at ScienceDirect

Frontiers in Laboratory Medicine

journal homepage: www.keaipublishing. com/FLM; www.frontlabmed.com

Pegylated doxorubicin gold complex: From nanovector to potential intercalant agent for biosensor applications

Valentina Melani [a], Maroua Ben Haddada [b], Hanane Moustaoui [b], Jessem Landoulsi [c], Nadia Djaker [b], Marc Lamy de la Chapelle [b,d], Jolanda Spadavecchia [b,*]

[a] Department of Experimental and Clinical Medicine, Section of Internal Medicine, University of Florence, Viale GB Morgagni 50, 50134 Florence, Italy
[b] CNRS, UMR 7244, CSPBAT, Laboratoire de Chimie, Structures et Propriétés de Biomateriaux et d'Agents Therapeutiques Université Paris 13, Sorbonne Paris Cité, Bobigny, France
[c] Sorbonne Universités, UPMC Univ Paris VI, Laboratoire de Réactivité de Surface, 4 place Jussieu, F-75005 Paris, France
[d] Southwest Hospital, Third Military Medical University, Chongqing, China

ARTICLE INFO

Article history:
Received 9 May 2017
Received in revised form 1 June 2017
Accepted 6 June 2017
Available online xxxx

Keywords:
Quartz Crystal Microbalance (QCM)
Chemical surface
DNA hybridization
Gold nanoparticles
Doxorubicin

ABSTRACT

We report an original approach to synthesize hybrid gold nanostructures in which doxorubicin (DOX), mixed to Poliethylenglycole diacid (PEG-COOH) led to original hybrid gold nanovector (DOX IN PEG AuNPs). In this work, we investigate the ability of DOX IN PEG-AuNPs to detect the amplification of the hybridization process by a sensitive Quartz crystal Microbalance with dissipation (QCM-D) by intercalation process. The sensing layer was carried out by self-assembled monolayer of β mercaptoethylamine (cysteamine) on gold-coated quartz crystal sensor composed by a rigid homobifunctional cross-linker 1,4 phenilenediisothiocyanate (PDITC) linked covalently with amino-probe oligonucleotides. By QCM characterization in the range from 8 μM to 20 nM, we demonstrate high specificity of DOX IN PEG-AuNPs-DNA with a limit of detection (LOD) of 9 nM. This result is very promising for development of sensitive and effective nanoparticle-based biosensor for quantifying small biomolecules concentration in physiological liquids. These results open a possibility to realize a new class of nanovector which will be tailored for different biomedical application, such as imaging, targeting and drugs delivery.

Introduction

Recently, great advances have been made in the use of gold nanoparticles (AuNPs), for biomedical applications, owing to their stability, chemical reactivity, non toxic nature, and scattering properties.[1–3] High biocompatibility, tunable surface chemistry and unique optical properties make nanogold a desirable platform for many biomedical and diagnostic applications.[4–6] For instance biomolecule- and/or biopolymer-conjugated AuNPs are largely used as biomarkers or biodelivery vehicles, as well as for cosmetics, as anti-aging components for skin protection.[7–9] In the last few years, many research works were devoted to the understanding of the effects of antitumor drugs on biological cells.[2,10] Other researchers have focused attention on small drugs that intercalate directly into the double helix of DNA as chemotherapeutic agents.[11] Doxorubicin is an anthracycline antibiotic. It is photosensitive and it works by intercalating DNA, while the most serious adverse effect is life-threatening heart damage.[12] A bulky sugar groups and a planar aglycon chromophore allows the insertion to the base pairs. The binding process hence induces large conformational deformations to the DNA helix, which in turn means that binding kinetics are slow.[13,14] The doxorubicin (DOX) has been conjugated to AuNPs (DOX-AuNPs) in order to improve the DOX therapeutic efficiency and the targeting of tumour cells reducing side effect but also to improve the imaging contrast or the photothermal cancer therapy.[15,16] Recently authors have demonstrated the ability of doxorubicin to be grafted on gold nanoparticles by carbodiimide chemistry. The so-called DOX-ON-PEG-AuNPs[17–19] were characterised by extinction spectroscopy (observation of the LSPR shift) and by Raman spectroscopy (observation of the band shift and of new Raman bands) to demonstrate the hybridization of the DOX to the AuNPs surface.[17,19]Successively H. Moustaouiet al. have designed a new nano-therapeutic agent based on a gold-DOX complex called DOX-IN-PEG-AuNPs.[20] Chemical-physical characterizations and biological "*in vitro*" studies, have fully elucidating that, the change of DOX conformation during the formation of gold-nanostructure by complexation have a large influence its therapeutic activity. The purpose of this study is to demonstrate the interaction of doxorubicin before (DOX *free*)

* Corresponding author.
E-mail address: jolanda.spadavecchia@univ-paris13.fr (J. Spadavecchia).

http://dx.doi.org/10.1016/j.flm.2017.06.004
2542-3649/

and after complexation of gold nanoparticles (DOX IN PEG-AuNPs) with duplex sequences oligonucleotides, expecting a better amplification of hybridization process during the intercalative process. The main advantages of QCM in sensing fields include high sensitivity, high stability, fast response and low cost. Under ideal conditions, the QCM technique, can detect mass changes of 1 ng/cm.[21] On the basis of the work of Sauerbrey[22], at 25 MHz, each shift of 1 Hz in the resonant frequency at the crystal corresponds to a mass change of 3.5 ng/cm.[2]

This remarkable mass sensitivity, has been exploited to study a variety of DNA based interactions including the detection of single base-pair mismatches during peptide nucleic acid-DNA hybridization[23,24], doxorubicin-DNA binding[25] and immobilization of DNA via a self-assembled monolayer of intercalative molecules.[26,27]To achieve detection of DOX free and DOX IN-PEG AuNPs to DNA (28mer) through a mass change, doxorubicin interact with DNA conjugated to a cross-linker cysteamine monolayer. A number of methods have been employed to bind DNA to surfaces for use in sensing devices such as localized surface plasmon resonance (LSPR)[19,28,29]and Raman spectroscopy.[17] The key to the application of the QCM technique to the study of biomolecular interactions is the formation of suitably immobilized biomolecular films. When considering the choice of immobilization method, the final desired coverage, molecular orientation, and point of DNA attachment are important factors.[30,31] Direct physical adsorption, complexation, cross-linking[32] and direct covalent attachment have all been employed.[17,20] The use of short alkanethiols linkages has the added benefit of placing the DNA strands close to the Quartz Crystal Microbalance sensor surface. Here we have chosen to immobilize first β mercaptoethylamine (cysteamine) on the gold electrodes of the crystal sensor. In a second step, the amino-groups on surface has been activated by 1,4phenilenediisothiocyanate (PDITC). Finally, amino-probe oligonucleotides has been linked covalently in order to monitored intercalation process after hybridization with doxorubicin-gold-nanoparticles (DOX IN PEG-AuNPs). For instance, force spectroscopy studies using the atomic force microscope (AFM-Tapping mode) were carried out to characterize the variation of gold surface morphology during intercalation experiments.

Experimental section

Materials

All chemicals were reagent grade or higher and were used as received unless otherwise specified. Tetrachloroauric acid ($HAuCl_4$), sodium borohydride ($NaBH_4$), Pyridine (98%), Dimethylformammide anhydrous (98%) ethanol (99%), 1,4phenylenediisothiocyanate (PDITC), sodium hydroxide (NaOH), phosphate buffered saline (PBS, 0.1 M, pH 7.4), dicarboxylic PolyEthylene Glycol (PEG)-600 (PEG), and doxorubicin hydrochloride (98%), were purchased from Sigma Aldrich. All solvents were used without any further purification. Experiments were carried out at room temperature if not specified otherwise.

Synthesis

Synthesis of pegylated- gold nanoparticles (PEG-Au NPs)

Synthetic procedures were carried out as previously described[18,19,34].

*Synthesis of doxorubicin-gold nanoparticles (**DOX IN PEG-Au NPs**)*

Synthetic procedures were carried out as recently described with some modifications.[20]

Briefly 20 ml $HAuCl_4$ aqueous solution ($2.5 * 10^{-4}$ M) was added to DOX (5 ml, $1.72 * 10^{-4}$ M in water) and aged for 10 min. After 10 min, 500 μl of dicarboxylic PEG was added and mixed by magnetic stirring for 10 min at room temperature. Finally, 20 ml of aqueous 0.01 M $NaBH_4$was added at -once. The as-prepared **DOX IN PEG-Au NPs** solution was centrifugated at 6.000 rpm for 20 min for three times and then the supernatant was discarded and the residue was redispersed in an equivalent amount of Buffer solution (PBS pH: 7). This was repeated twice principally to remove excess of doxorubicin and PEG diacid. Stock solutions were stored at 27–29 °C and characterized using UV–Vis spectroscopy and transmission electron microscopy (TEM).

Intercalation of doxorubicin pegylated-Au nanoparticles to DNA in solution (DNA-DOX-IN-PEG-Au NPs)

The intercalation process between doxorubicin-pegylated-gold nanoparticles and DNA oligonucleotides was conducted at room temperature under ionic conditions. 200 μL of **DOX IN PEG-Au NPs** solution (20 nM in 0.1 M PBS) was treated with 30 μL of 10% NaCl. After this process, 40 μL of 100 nM H_2N-DNA (probe1) and the complementary strands (target1), were added onto the **DOX IN PEG-Au NPs** solution for 4 h at room temperature in PBS buffer (1 M NaCl, 100 mM phosphate buffer, pH 7). The resultant colloidal solution was stirred for 1 h at room temperature and characterized by UV–Visible absorption and TEM.

DNA hybridization

For end-point measurement, the surface was exposed to the complementary targets (labelled and non-labelled) at 21 °C during 1 h in a hybridization chamber at pH 7. The denaturation of hybridized DNA was performed using NaOH (1 mM) during 1 min followed with rinsing with PBS.

Intercalation of DOX and DOXIN-PEG-AuNPs with DNA stabilized PEG-AuNPs

50 μl of an aqueous solution of doxorubicin, was added into 5 mL of DNA stabilized PEG-AuNPs for 2 h. This experiment was repeated with DOX IN-PEGAuNPs and the intercalation processes were recorded at a precise short interval time by UV VIS absorption spectra and then confirmed by QCM-D measurements.

QCM substrate preparation

The schematic diagram of the chemical immobilization method is depicted in Scheme 1. The chemical procedures for the formation of a cysteamine SAM on the planar gold surface, and the binding of the PDITC linker in absolute ethanol have been described previously[32].

The 28^{mer} oligonucleotides were purchased from Eurogentec and have the following sequences:

- DNA oligonucleotides on QCM surface (probe 1): 5′-H_2N-TTT-TGG-GAT-GGT-TGA-GGG-TGC–CTC-TGG-C-3′.
- Complementary DNA in solution (target 1): 5′-GCC-AGA-GGC-ACC–CTC-AAC-ACT-CCC-A3′.

Similar solutions of non complementary oligonucleotides and “free” pegylated gold nanoparticles (PEG-AuNPs), were prepared as control for all experiments. For drug binding study, doxorubicin (DOX) solution (4 and 8 μg/ml) was prepared in PBS buffer (1 M NaCl, 100 mM phosphate buffer, pH 7). All solutions were filtered and sterilized prior to use.

Please cite this article in press as: Melani V., et al. Pegylated doxorubicin gold complex: From nanovector to potential intercalant agent for biosensor applications Frontiers in Laboratory Medicine (2017), http://dx.doi.org/10.1016/j.flm.2017.06.004

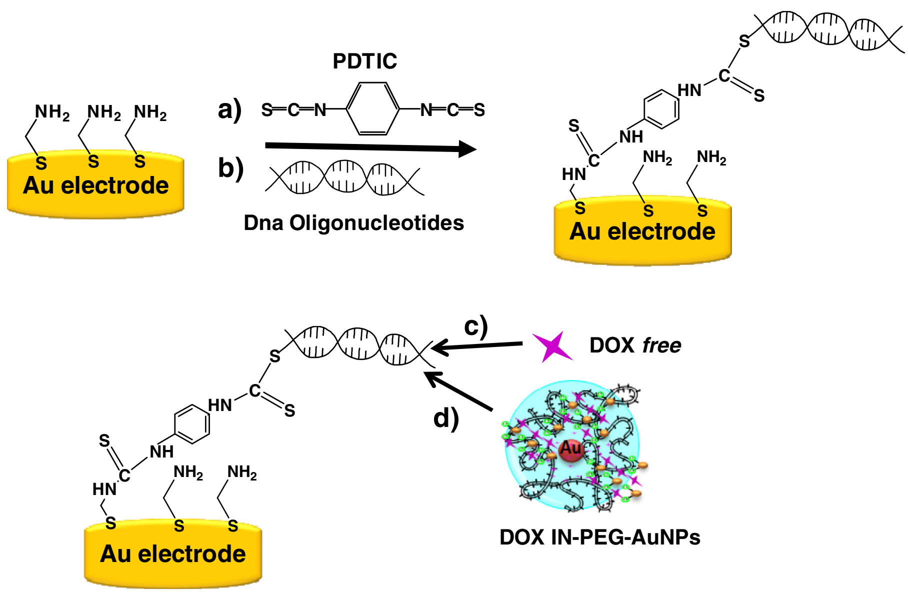

Scheme 1. Schematic reaction mechanism for the covalent attachment of DNA oligonucleotides to a gold surface (a) initial SAMs of cysteamine and covalent attachment of PDTIC (b) cross linking of H_2N-terminated oligonucleotides and complementary target (c) Intercalation of doxorubicin free (DOX) (d) and pegylated doxorubicin gold nanoparticles (DOXO IN-PEG-AuNPs).

SAM formation and activation of PDITC

The sensor chip were dipped in a freshly prepared solution of cysteamine (10 mM in water) for 18–24 h. After washing, with water, they were further dipped in a solution of PDITC (0.02% w/v in pyridine/DMF 1:9) for 2 h. The sensors were extensively washed in absolute ethanol two times and dried under a flow argon.[32]

DNA sensor construction

An activated sensor was mounted in the QCM and a solution of H_2N DNA (c: 100 nM in PBS) was flowed for 100 min. After a washing step with PBS, the hybridization step, with DNA target (c: 50 nM in PBS) was applied for 100 min. The following protocol was used to link DNA molecules (probe 1) on the PDC-terminated surface. 20 μL of DNA probe 1 (100 nM in PBS buffer (0.1 M, pH 7.4)) was added onto a cysteamine-terminated surface. A cover-chip was placed on top of the drop and allowed to incubate for 3 h at 4 °C. The DNA-immobilized on gold quartz surface was washed three times in water and then immersed in water for subsequent hybridization.

Detection of doxorubicin (DOX) in the direct assay format

Solutions of DOX (from at 8 μM to 20 nM) were prepared in PBS from the stock aqueous solution. These solutions were flowed over chip for 30 min followed by a washing step with PBS for 5 min. The variation of frequency between the beginning of injection and the end of the washing step was measured on each sensorgram.

Detection of DOX IN-PEG AuNPs in the direct assay format

A solution of DOX IN-PEG AuNPs (c: (from at 8 μM to 20 nM)) was flowed over the sensor after hybridization process for 150 min, followed by a washing step with PBS for 5 min, and regeneration step by NaOH (1 mM in water) for 1 min during three times.

Instrumentation

UV/Visisble absoprtion measurements

Absorption spectra were recorded using a Perkin Elmer Lambda UV/Vis 950 spectrophotometer in plastic cuvettes with an optical path of 10 mm. The wavelength range was 400–800 nm.

Transmission electron microscopy (TEM)

Transmission electron microscopy imaging was performed using a JEOL JEM 1011 microscope operating at an accelerating voltage of 100 kV. The TEM images were taken after separating the surfactant from the metal particles by centrifugation. Typically 1 mL of the sample was centrifuged for 21 min at a speed of 6.000 rpm. The upper part of the colorless solution was removed and the solution fraction was re-dispersed in 1 mL buffer solution (PBS, pH 7). 2 μL of this re-dispersed particle suspension was placed on a carbon-coated copper grip and dried at room temperature.

AFM

AFM images were recorded in Peak Force Tapping™ mode.[33] In this mode, the z-piezo, modulated far below the cantilever resonance frequency, performs very fast approach-retracting curves at each pixels of the image. The peak interaction forces obtained is thus used as the imaging feedback signal, allowing the applied force to be lower than in normal tapping mode. Oxide-sharpened microfabricated Si_3N_4 cantilevers (Microlevers, Veeco Metrology LLC, Santa Barbara, CA) with a spring constant of 0.36 N/m (as verified with the thermal noise method) and a curvature radius of ~10 nm, were used at a scan rate of 1–2 Hz. The cantilever top was coated with a thin Ti–Al layer to enhance the laser reflection during the fast cantilever oscillation. Images were obtained at room temperature (20–22 °C) in air. All images shown in this paper are flattened raw data.

QCM-D measurements

QCM-D is a powerful detection technique to study viscoelastic monolayer, biofilm and small proteins in liquid.[11] Experiments were performed using a dissipative Quartz Crystal Microbalance setup (QSense, Sweden). A temperature controlled 400 μL static cell was used to submit the functionalised gold surfaces to the various solutions of proteins. The QCM-D device was temperature – controlled at 22 °C; this QCM-D set up allows the simultaneous recording of resonance frequency and dissipation between the

Please cite this article in press as: Melani V., et al. Pegylated doxorubicin gold complex: From nanovector to potential intercalant agent for biosensor applications Frontiers in Laboratory Medicine (2017), http://dx.doi.org/10.1016/j.flm.2017.06.004

two electrodes of the quartz crystal. The crystal were treated prior to UV-light for 20 min to remove organic contamination and then rinsed by immersion in ethanol absolute and milliQ water and dried under a stream of nitrogen. The kinetics of sample adsorption and desorption were followed by changes in the resonant frequency on the crystal and dissipation of the crystal vibrations. In liquid environments, the limit for the mass sensitivity was on the order of 5 ng/cm^2, and the dissipation factor (D) was approximately $3 \cdot 10^{-7}$ for the unloaded 5 MHz crystal. The crystal resonant frequency shift (Δf) and the dissipation factor (ΔD) of the oscillator were measured simultaneously at the fundamental resonant frequency (5 MHz) and at a number of overtones including 25 MHz (used for the data presented here). Mass uptakes Δm were calculated with Sauerbrey Eq. (1) assuming the deposited films be have as an elastic mass:

$$\Delta F = -N \times \Delta m / C_f \quad (1)$$

where ΔF is the frequency shift at the 5th overtone, C_f (=−17.7 ng/cm^2/Hz at F = 5 MHz) the mass sensitivity factor and N (=5) the overtone number.

For adsorption of DNA Oligonucleotides onto a bare surface, the sample solution were pumped through the flow cell by a peristaltic pump at a flow 100 μL/min. Desorption was performed immediately after adsorption reached steady state, by replacing the protein solution with a pure buffer flow. Measuring the final frequency change in the presence of pure buffer (referred to the baseline in buffer) means that oligonucleotides adsorption is found without involving changes in the liquid density and viscosity.

Results and discussion

Synthesis and characterization of pegylated doxorubicin-gold nanoparticles (DOX-IN-PEG- NPs)

Recently, H. Moustaoui et al. have designed a novel method to graft DOX on gold nanoparticles via complexation of gold ions in order to improve the therapeutic effect of the drug in pancreatic cancer cells (PDAC).[20] The synthesis of pegylated doxorubicin-gold nanoparticles (DOX IN-PEG-AuNPs) was achieved by reducing tetrachloroauric acid ($HAuCl_4$) with sodium borohydride ($NaBH_4$) in the presence of PEG (dicarboxylic polyethylenglicole) and DOX (doxorubicin hydrochloride) as capping agents. (Fig. 1) The main difference with other synthetic procedures of DOX-Au NPs is that doxorubicin hydrochloride is used in the same way as citrate for the stabilisation of the particles through electrostatic interactions between the carboxylic acid groups and the gold surface[20] forming a complex between the DOX and the Au.

DOX IN-PEG-AuNPs absorption spectrum exhibits a peak centered at 520 nm as described previously (Fig. 1-PANEL A-red-line). This latter peak is assigned to the localised surface plasmon of the nanoparticle with diameter of 8 nm embedded in PEG environment as expected.[35] In order to evaluate the intercalation effect between DOX-IN-PEG-AuNPs, and DNA oligonucleotides, in solution, a buffer solution composed by double strand DNA at different concentrations (from 5 μM to 20 nM) were mixed with DOX IN-PEG-AuNPs under ionic conditions (PBS, NaCl 0.5 Mm, pH 7). After interaction of DOX IN-PEG-AuNPs (Fig. 1-PANEL A-black-line) with oligonucleotides, a dramatic red-shift from 520 to 636 nm is observed confirming the formation of a DOX-DNA complex and the resulting solution was colourless. We suggest that this change was associated to the successful intercalation of the DOX within the double DNA strands, and as a consequence to the AuNPs aggregation associated to the formation of van der Waals oligonucleotides interactions among particles.[36] This means that even if the DOX is grafted at the nanoparticle surface, it is still able to interact with the DNA double strand. The morphology of DOX IN-PEG-AuNPs (Fig. 1-PANEL B-left-image), as revealed by TEM, was spherical and well defined, with AuNPs of homogenous shape. Following intercalation process with oligonucleotides, DOX IN-PEG-AuNPs formed highly ordered clustered aggregates as chains (Fig. 1-PANEL B-right-image), due to the electrostatic interaction between the phosphate groups of oligonucleotides and the PEG-diacid molecules at the gold particles surface.

DOX-DNA hybridization dynamic observed by QCM

The interaction between DNA and DOX IN-PEG-AuNPswas investigated on flat gold substrate by means of QCM-D and AFM. For this purpose, DNA and its target were immobilized on modified QCM gold electrode following the strategy depicted in Scheme 1.

In previous study, Spadavecchia et al., have demonstrated the versatility of this chemistry onto a gold surface previously functionalized by neutravidin onto PDTIC layer and biotinylated probe in order to monitored the hybridization DNA process.[32] In this case, the amino-probe was actively grafted onto PDTIC–cysteamine-self-assembled monolayer, without supplementary chemical step As previously described, PDTIC offers some specific advantages as the efficient cross-linking of terminated amino-group that allows the covalent attachment of various biomolecules and small organic compounds.[37]

In Fig. 2 we observed the process of immobilization of amino-oligonucleotide (probe) during 100 min that induces a significative variation of frequence (Δf = 26 Hz) with a very low kinetic of adsorption. This phenomena probably depends on the hindrance steric conformation of the DNA probe (28mer), the grafting density, and the structural chemistry rigidity of SAM onto gold surface. A frequency shifts is observed after diffusion of target oligonucleotides in PBS solution (pH 7.2), when the solution was injected during 75 min. The very loss dissipation shifts observed here, suggests that, the covalent bound oligonucleotides, form a rigid film at the surface[11] as required for the valid application of the Saurbrey equation. Furthermore the layer thickness is in the range of the Saurbrey relation validity and hence we use this approach here. Therefore, the shift of −21 Hz observed at time 250 min (after hybridization of target and PBS washing) corresponds to a mass deposition of 372 ng * cm^{-2} and an estimate of 3.7 * 10^{12} of duplex strands formed per square centimeter at the QCM electrode surface. Each exposition was washed by PBS to remove oligonucleotides molecules in excess. After first intercalation of pure DOX (4 μM), the Δf was stable (Δf = −23 Hz after PBS washing/-time 310 min) meaning that nearly no DOX molecule interacts with the DNA double strands. Next exposition with a double concentration of DOX, showed a dramatic decrease of frequency not stable after washing with PBS; the frequency is −25 Hz. This low variance is due to a saturation of the intercalation sites after the first passage of doxorubicin and the steric hindrance reduce the potential number of binding of the drugs. Some experiments were carried out directly with a SAM-oligonucleotides and monitoring the hybridization process with a complementary target and DOX *free* (Fig. 3). After hybridization process, the regeneration step to dissociate DNA linkage performed in a solution of NaOH (1 mM) was very efficient to detach complementary target in order to confirm the reproducibility of the experiments.

The variation of the frequency of the quartz and the dissipation resulting from the adsorption of DOX IN PEG-AuNPs on duplex (probe and target) are presented in the Fig. 4. As expected, the injection of DOX IN PEG-AuNPs resulted in significant negative shifts of the resonance frequency and concomitant increase of the dissipation owing to mass uptake. After rinsing with PBS, the frequency shift is equal to −32 Hz. To verify the specificity of the

Please cite this article in press as: Melani V., et al. Pegylated doxorubicin gold complex: From nanovector to potential intercalant agent for biosensor applications Frontiers in Laboratory Medicine (2017), http://dx.doi.org/10.1016/j.flm.2017.06.004

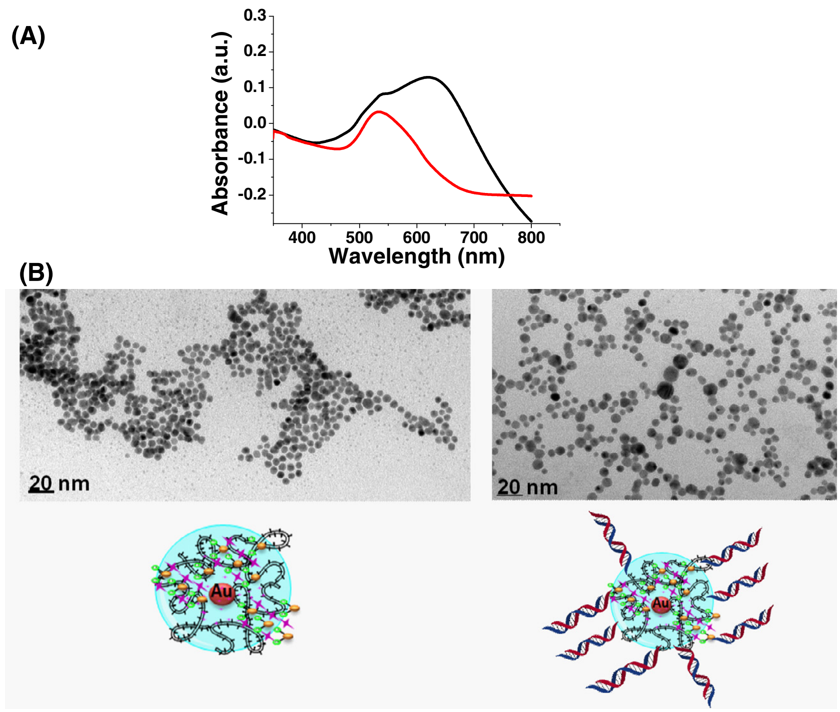

Fig. 1. PANEL A: UV VIS spectroscopy of the SPR band changes of pegylated doxorubicin gold nanoparticles (DOX IN PEG-AuNPs) before (red-line) and after dsDNA/ssDNA oligonucleotides intercalation (black line) PANEL B: TEM images of a solution of DOX IN PEG-AuNPs as synthetized (left image) and after intercalation dsDNA/ssDNA oligonucleotides intercalation (right image) forming linear chains.

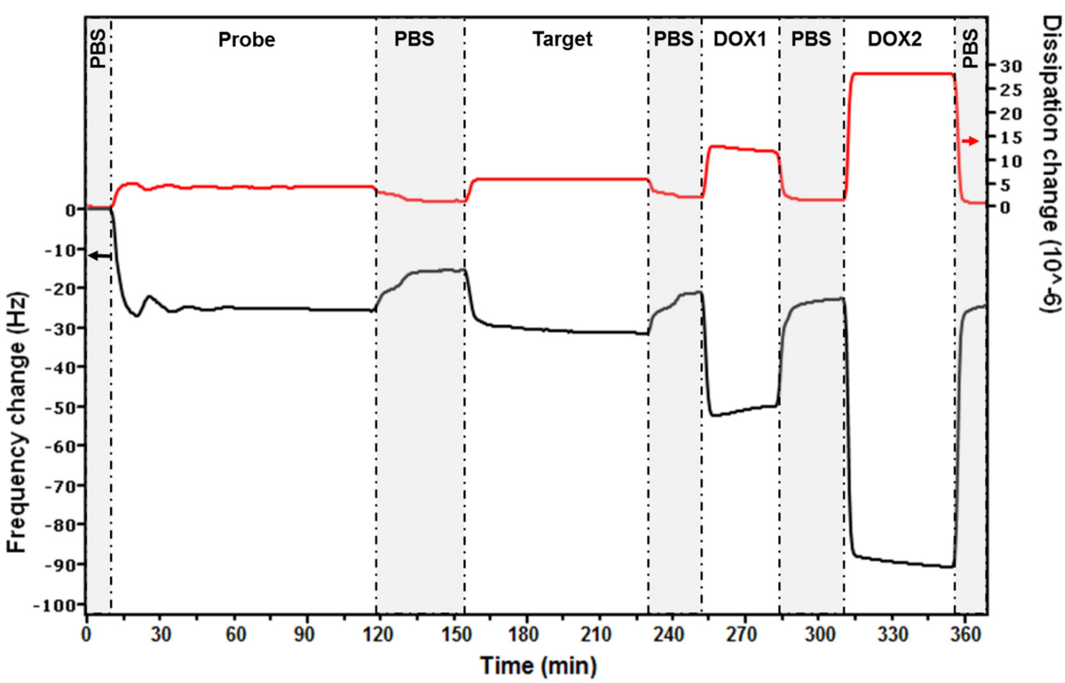

Fig. 2. QCM-D measurements and real-time monitoring of different concentrations of DOX *free* (DOX1 = 4 μM and DOX2 = 8 μM) by a cysteamine modified gold substrate showing frequency changes in the 5th overtone (black line) and the corresponding dissipation change (red line) vs. time during the intercalation onto ds DNA/ssDNA oligonucleotides.

nanovector during hybridization if the adsorption of AuNPs was specific, a gold substrate functionalized with cysteamine, PDITC and single stranded of DNA (probe) was exposed to a complementary DNA (target) solution. Following the hybridization, the surface was treated with a colloidal solution of PEG-AuNPs (without DOX). The variation of frequency is presented in Fig. S1. Initially we observe an initial mass deposition on quartz surface, measured through the variations of frequency. However, after washing with PBS, the frequency value is returned to zero, demonstrating that all the mass deposited on the quartz has been removed. This phenomenon, has confirmed that, the process of stable interaction of PEG-AuNPs with the double helices of DNA is mediated by the

Please cite this article in press as: Melani V., et al. Pegylated doxorubicin gold complex: From nanovector to potential intercalant agent for biosensor applications Frontiers in Laboratory Medicine (2017), http://dx.doi.org/10.1016/j.flm.2017.06.004

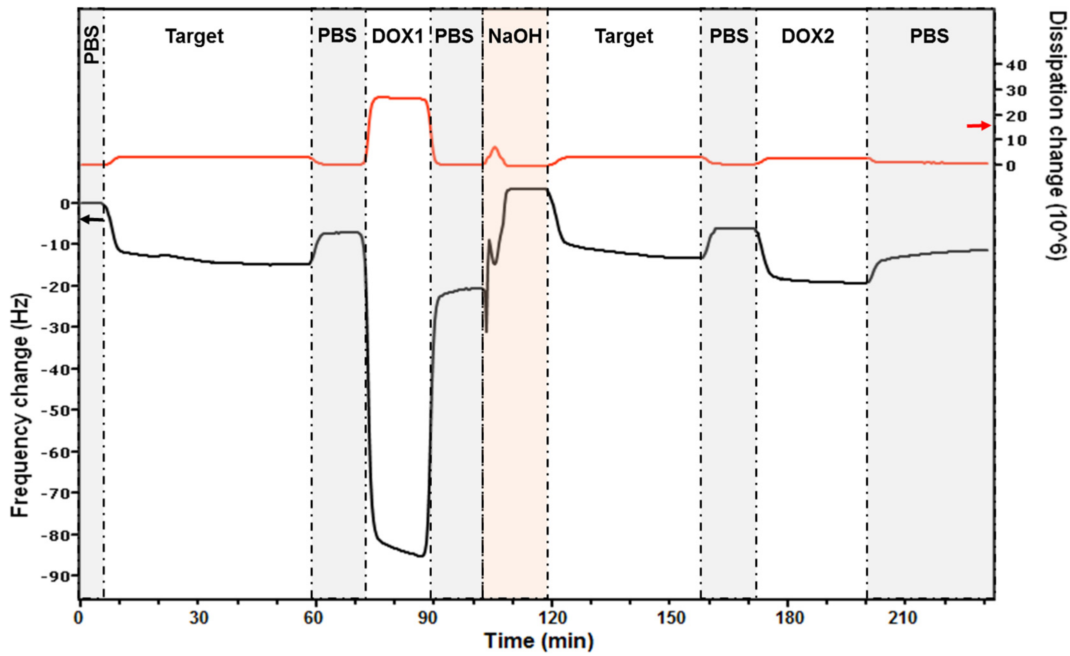

Fig. 3. QCM-D measurements and real-time monitoring of different concentrations (4, 8 μM) of DOX *free* by a cysteamine modified gold substrate with amino-probe via PDITC showing frequency changes in the 5th overtone (black line) and the corresponding dissipation change (red line) vs. time during the intercalation onto ds DNA/ssDNA oligonucleotides.

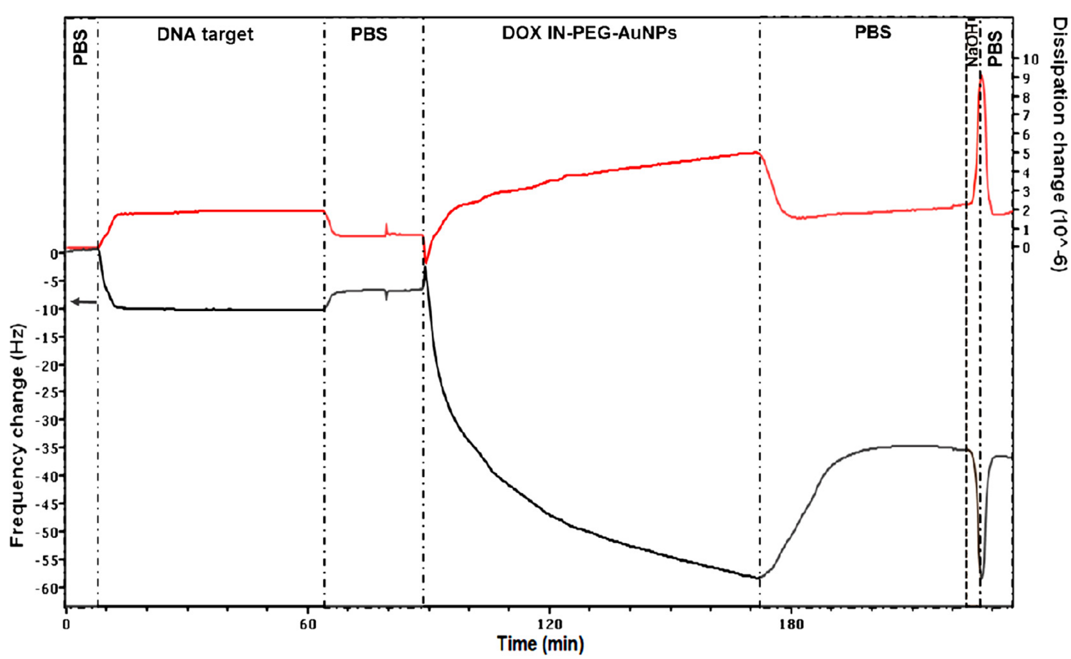

Fig. 4. QCM-D measurements and real-time monitoring of different concentrations (4, 8 μM) of DOX IN PEG-AuNPs by a cysteamine modified gold substrate with amino-probe via PDITC showing frequency changes in the 5th overtone (black line) and the corresponding dissipation change (red line) vs. time during the intercalation onto ds DNA/ssDNA oligonucleotides.

DOX molecules linked to its surface. The total of the mass removed is also attributable to electrostatic repulsion between the negative charges of the DNA and carboxyl group of the PEG onto AuNPs.

In order to determine the sensitivity reached by SAMs-oligonucleotides based nanodevices, QCM measurements of intercalation were performed at various DOX and DOX IN PEG-AuNPs concentrations, from 20 nM to 8 μM. Therefore calibration (dose–response) curves were established by plotting $-\Delta F$ as a function of DOX concentration (Fig. 5). Curve-fitting of data with the Langmuir isotherm Eq. (2) assuming independent and equivalent surface binding sites gave correlation coefficients higher than 0.9.

$$\Delta F = \Delta F_{max} \times [DOX]/([DOX] + K) \quad (2)$$

with K the association constant.

The piezoelectric sensor thus set up was able to detect and quantify DOX in the range between 20 nM to 8 μM. The limit of detection was calculated on the basis of a response $\Delta F = -1$ Hz,

Please cite this article in press as: Melani V., et al. Pegylated doxorubicin gold complex: From nanovector to potential intercalant agent for biosensor applications Frontiers in Laboratory Medicine (2017), http://dx.doi.org/10.1016/j.flm.2017.06.004

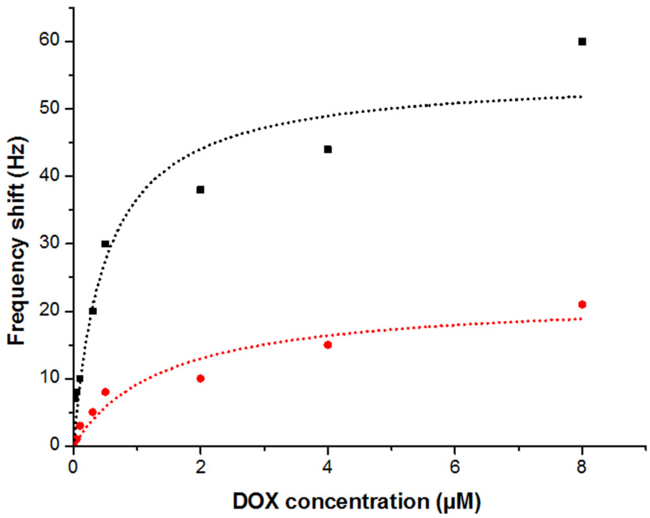

Fig. 5. Quartz frequency variation vs DOX concentration free (red) and complexed onto gold nanoparticles DOX IN PEG-AuNPs (black) and mathematical curve fitting according to the Langmuir equation ($-\Delta F = 22 \times [DOX]/[DOX] + 1.4$, $r = 0.93$) and ($-\Delta F = 55 \times [DOX]/[DOX] + 0.5$, $r = 0.94$) respectively.

is equal to 67 and 9 nM for DOX free and DOX IN PEG-AuNPs respectively.

Determination of the number of gold nanoparticles deposited at the QCM surface

In order to determine the number of gold nanoparticles deposited at the QCM electrode surface, we have estimated their mass, *m*.

In this case, we assume that they have spherical shape. *m* can be calculated using the following equation:

$$m = \frac{4}{3}\pi r^3 \rho$$

with *r* the nanoparticle radius ($r = 3.5$ nm) and ρ is the density of the gold ($\rho = 19.3\ g\ cm^{-3}$).

The distribution of the nanoparticle size gives an average diameter of 7 nm and thus an average mass of $3.466 \cdot 10^{-21}$ kg (we assume that the mass of the molecules as the DOX grafted at the nanoparticle surface is negligible).

As the frequency shift is of 32 Hz at a concentration of 4 µM, one can estimate a mass deposition of 567 ng/cm^2 and thus a number of $1.63 \cdot 10^{11}$ nanoparticles/cm^2 at the QCM electrode surface.

Since the number of DNA duplex strands at the surface is $3.7 \cdot 10^{12}$/cm^2, it means that we have 1 nanoparticle for 20 duplex strands. One can also assume that one nanoparticle is covered by several DOX molecules and that one nanoparticle interacts with several duplexes (maximum 4 duplex strands as the average distance between two duplex strands can be estimated to be close to 5 nm). For comparison, with a frequency shift of 1 Hz for the pure DOX molecule, one can estimate an interaction of 5 DOX molecules with one duplex strand.

Interaction on flat substrate (AFM)

AFM images revealed the presence of well defined nanoparticles highly dispersed on the gold surface in comparaison with AFM height images of DNA-modified gold surfaces (Fig. S2-A) after immobilization and successive hybridization of DNA target and further treatment with (Fig. S2-B) doxorubicin free (DOX). The NPs are either isolated or much closed to each other, but only few aggregates can be observed on the surface (Fig. S2-Band D) The NPs density, evaluated using a statistical analysis of $1 \times 1\ \mu m^2$ image, yields an average of about 1.4×10^{14} NPs per square centimeter. Regarding the NPs size, cross sections indicated that the particles are homogenous (particle height near 8 nm, Fig. 4C). When the particles were in close contact with each other, the AFM tip was too large to probe the interstices between particles but, the real particle height could be evaluated reliably (Fig. S2-C). Accordingly, based on cross sections, a height size distribution analysis can be made. Results given in Fig. S2-D show a NPs size of 8 nm ± 0.4 nm in diameter, in agreement with observations made with TEM microscopy.

Conclusion

We have demonstrated the potential of detecting duplex formation for short lengths of oligonucleotides and subsequent DOX IN PEG-AuNPs into molecule-DNA intercalation using the QCM technique with a decrease of the detection limit to 9 nM. The different steric arrangement of DOX into nanoparticles reveals a potential power of intercalation during hybridization events. We believe that this technique open the possibility to detect various biophysical interaction between biomolecules of interest in the field of Nanomedicine.

Acknowledgment

The Laboratoire de Reactivitè de Surface (LRS), the Centre National de la Recherche Scientifique (CNRS), are gratefully acknowledged for financial support.

Appendix A. Supplementary data

Supplementary data associated with this article can be found, in the online version, at http://dx.doi.org/10.1016/j.flm.2017.06.004.

References

1. Huang X, El-Sayed MA. Gold nanoparticles: optical properties and implementations in cancer diagnosis and photothermal therapy. *J Adv Res*. 2010;1(1):13–28.
2. Jiang S, Win KY, Liu S, Teng CP, Zheng Y, Han M-Y. Surface-functionalized nanoparticles for biosensing and imaging-guided therapeutics. *Nanoscale*. 2013;5(8):3127–3148.
3. Retif P, Pinel S, Toussaint M, et al. Nanoparticles for radiation therapy enhancement: the key parameters. *Theranostics*. 2015;5.
4. Shah M, Badwaik VD, Dakshinamurthy R. Biological applications of gold nanoparticles. *J Nanosci Nanotechnol*. 2014;14(1):344–362.
5. McQuaid HN, Muir MF, Taggart LE, et al. Imaging and radiation effects of gold nanoparticles in tumour cells. *Sci Rep*. 2016;6:19442.
6. Meyers JD, Cheng Y, Broome AM, et al. Peptide-targeted gold nanoparticles for photodynamic therapy of brain cancer. *Part Part Syst Charact*. 2015;32.
7. Gupta S, Bansal R, Gupta S, Jindal N, Jindal A. Nanocarriers and nanoparticles for skin care and dermatological treatments. *Indian Dermatol Online J*. 2013;4 (4):267–272.
8. Lohani A, Verma A, Joshi H, Yadav N, Karki N. Nanotechnol Based Cosmeceuticals. *ISRN Dermatol*. 2014;2014:843687.
9. Li C, Li D, Wan G, Xu J, Hou W. Facile synthesis of concentrated gold nanoparticles with low size-distribution in water: temperature and pH controls. *Nanoscale Res Lett*. 2011;6(1). 440-440.
10. Chithrani BD, Ghazani AA, Chan WC. Determining the size and shape dependence of gold nanoparticle uptake into mammalian cells. *Nano Lett*. 2006;6.
11. Pope LH, Allen S, Davies MC, Roberts CJ, Tendler SJB, Williams PM. Probing DNA duplex formation and DNA−drug interactions by the quartz crystal microbalance technique. *Langmuir*. 2001;17(26):8300–8304.
12. Cui T, Liang JJ, Chen H, et al. Performance of doxorubicin-conjugated gold nanoparticles: regulation of drug location. *ACS Appl Mater Interfaces*. 2017;1 (10).
13. Temperini C, Messori L, Orioli P, Bugno CD, Animati F, Ughetto G. The crystal structure of the complex between a disaccharide anthracycline and the DNA hexamer d(CGATCG) reveals two different binding sites involving two DNA duplexes. *Nucleic Acids Res*. 2003;31(5):1464–1469.

Please cite this article in press as: Melani V., et al. Pegylated doxorubicin gold complex: From nanovector to potential intercalant agent for biosensor applications Frontiers in Laboratory Medicine (2017), http://dx.doi.org/10.1016/j.flm.2017.06.004

14. Yang X-L, Wang AHJ. Structural studies of atom-specific anticancer drugs acting on DNA. *Pharmacol Therapeutics*. 1999;83(3):181–215.
15. Banu H, Sethi DK, Edgar A, et al. Doxorubicin loaded polymeric gold nanoparticles targeted to human folate receptor upon laser photothermal therapy potentiates chemotherapy in breast cancer cell lines. *J Photochem Photobiol B*. 2015;149:116–128.
16. Liao J, Li W, Peng J, et al. Combined cancer photothermal-chemotherapy based on doxorubicin/gold nanorod-loaded polymersomes. *Theranostics*. 2015;5 (4):345–356.
17. Spadavecchia J, Perumal R, Casale S, Krafft J-M, Methivier C, Pradier C-M. Polyethylene glycol gold-nanoparticles: Facile nanostructuration of doxorubicin and its complex with DNA molecules for SERS detection. *Chem Phys Lett*. 2016;648:182–188.
18. Spadavecchia J, Movia D, Moore C, et al. Targeted polyethylene glycol gold nanoparticles for the treatment of pancreatic cancer: from synthesis to proof-of-concept in vitro studies. *Int J Nanomed*. 2016;11:791–822.
19. Spadavecchia J, Perumal R, Barras A, et al. Amplified plasmonic detection of DNA hybridization using doxorubicin-capped gold particles. *Analyst*. 2014;139 (1):157–164.
20. Moustaoui H, Movia D, Dupont N, et al. Tunable design of gold(III)–doxorubicin complex–pegylated nanocarrier. the golden doxorubicin for oncological applications. *ACS Appl Mater Interfaces*. 2016;8(31):19946–19957.
21. Politi J, Rea I, Nici F, et al. Nanogravimetric and optical characterizations of thrombin interaction with a self-assembled thiolated aptamer. *J Sensors*. 2016;2016:8.
22. Sauerbrey G. Verwendung von Schwingquarzen zur Wägung dünner Schichten und zur Mikrowägung. *Zeitschrift für Physik*. 1959;155(2):206–222.
23. Dunn KE, Trefzer MA, Johnson S, Tyrrell AM. Investigating the dynamics of surface-immobilized DNA nanomachines. *Sci Rep*. 2016;6:29581.
24. Wang J. From DNA biosensors to gene chips. *Nucleic Acids Res*. 2000;28 (16):3011–3016.
25. Pengyang W, Xin W, Liming W, Xiaoyang H, Wei L, Chunying C. Interaction of gold nanoparticles with proteins and cells. *Sci Technol Adv Mater*. 2015;16 (3):034610.
26. Sakao Y, Nakamura F, Ueno N, Hara M. Hybridization of oligonucleotide by using DNA self-assembled monolayer. *Colloids Surf B Biointerfaces*. 2005;40(3–4):149–152.
27. Zhao W, Lam JC, Chiuman W, Brook MA, Li Y. Enzymatic cleavage of nucleic acids on gold nanoparticles: a generic platform for facile colorimetric biosensors. *Small*. 2008;4(6):810–816.
28. Spadavecchia J, Barras A, Lyskawa J, et al. Approach for plasmonic based DNA sensing: amplification of the wavelength shift and simultaneous detection of the plasmon modes of gold nanostructures. *Anal Chem*. 2013;85(6):3288–3296.
29. Zagorodko O, Spadavecchia J, Serrano AY, et al. Highly sensitive detection of DNA hybridization on commercialized graphene-coated surface plasmon resonance interfaces. *Anal Chem*. 2014;86(22):11211–11216.
30. Samanta D, Sarkar A. Immobilization of bio-macromolecules on self-assembled monolayers: methods and sensor applications. *Chem Soc Rev*. 2011;40 (5):2567–2592.
31. Roy D, Park JW. Spatially nanoscale-controlled functional surfaces toward efficient bioactive platforms. *J Mater Chem B*. 2015;3(26):5135–5149.
32. Spadavecchia J, Moreau J, Hottin J, Canva M. New cysteamine based functionalization for biochip applications. *Sensors Actuators B: Chem*. 2009;143 (1):139–143.
33. Möller C, Allen M, Elings V, Engel A, Müller DJ. Tapping-mode atomic force microscopy produces faithful high-resolution images of protein surfaces. *Biophys J*. 1999;77(2):1150–1158.
34. Politi J, De Stefano L, Rea I, et al. One-pot synthesis of a gold nanoparticle-Vmh2 hydrophobin nanobiocomplex for glucose monitoring. *Nanotechnology*. 2016;27(19):0957–4484.
35. Song J, Niu G, Chen X. Amphiphilic-polymer-guided plasmonic assemblies and their biomedical applications. *Bioconjug Chem*. 2017;28(1):105–114.
36. Orendorff CJ, Hankins PL, Murphy CJ. PH-triggered assembly of gold nanorods. *Langmuir*. 2005;21(5):2022–2026.
37. Zimmermann JL, Nicolaus T, Neuert G, Blank K. Thiol-based, site-specific and covalent immobilization of biomolecules for single-molecule experiments. *Nat Protocols*. 2010;5(6):975–985.

Please cite this article in press as: Melani V., et al. Pegylated doxorubicin gold complex: From nanovector to potential intercalant agent for biosensor applications Frontiers in Laboratory Medicine (2017), http://dx.doi.org/10.1016/j.flm.2017.06.004